

Search for new physics in $b \rightarrow s\ell^+\ell^-$ transitions at CMS

Alessio Boletti^{a,*} on behalf of the CMS Collaboration

^a*Laboratório de Instrumentação e Física Experimental de Partículas (LIP)*

Av. Gama Pinto 2, Lisbon, Portugal

E-mail: alessio.boletti@cern.ch

The flavour-changing neutral current decays are interesting probes for new physics searches. The angular distributions of the $B^+ \rightarrow K^{*+}\mu^+\mu^-$ decay is studied using a sample of proton-proton collisions at $\sqrt{s} = 8$ TeV collected with the CMS detector at the LHC, corresponding to an integrated luminosity of 20.5 fb^{-1} . An angular analysis is performed to determine the longitudinal polarisation fraction and the muon forward-backward asymmetry, as functions of the dimuon invariant mass squared. All the measurements are consistent with the standard model predictions. In addition, the projections for the sensitivity of the measurement of the P'_5 parameter in the $B^0 \rightarrow K^{*0}\mu^+\mu^-$ angular analysis that is foreseen to be performed on the data that CMS will collect at the High-Luminosity LHC is reported.

40th International Conference on High Energy physics - ICHEP2020

July 28 - August 6, 2020

Prague, Czech Republic (virtual meeting)

*Speaker

1. Introduction

Phenomena beyond the Standard Model (SM) can be probed directly, via the production of new particles, or indirectly, by studying the production and decay of SM particles. The transitions of the type $b \rightarrow s\ell^+\ell^-$ are flavour-changing neutral current (FCNC) processes. According to the SM, these transitions are forbidden at tree level and occur through higher-order penguin or box diagrams. For this reason, the measurement of these rare FCNC decays is very sensitive to physics phenomena beyond the SM.

The Compact Muon Solenoid Experiment (CMS) [1] has analysed three FCNC decays: $B^0 \rightarrow K^{*0}\mu^+\mu^-$ [2, 3], $B^+ \rightarrow K^+\mu^+\mu^-$ [4], and $B^+ \rightarrow K^{*+}\mu^+\mu^-$ [5]. All these analyses use a data sample collected in proton-proton (pp) collisions at a centre-of-mass energy of 8 TeV with the CMS detector at LHC, corresponding to an integrated luminosity of 20.5 fb^{-1} . In this report the most recent analysis of the $B^+ \rightarrow K^{*+}\mu^+\mu^-$ decay is presented¹. In addition, the projection of the analysis of the neutral channel on the data that will be collected by CMS in the HL-LHC data-taking is reported.

2. The $B^+ \rightarrow K^{*+}\mu^+\mu^-$ decay [5]

The angular distribution of the process $B^+ \rightarrow K^{*+}\mu^+\mu^-$ can be described as a function of four kinematic variables: the dimuon invariant mass, q^2 , the decay angle of the dimuon system, θ_ℓ , the decay angle of the K^{*+} , θ_K , and the angle between these two decay planes, ϕ . The K^{*+} meson is reconstructed through its decay $K^{*+} \rightarrow \pi^+K_s^0$ and the K_s^0 in its decay to two charged pions.

Due to the limited yield of signal events observed in the collected dataset, a full three-dimensional angular analysis was not possible. Since the two angular parameters with the largest physical interest, the fraction of longitudinally polarised K^{*+} , F_L , and the muon forward-backward asymmetry, A_{FB} , do not depend on the angular variable ϕ , this angle is integrated out.

The θ_ℓ and θ_K dependence of the decay rate can be parameterised in terms of F_L and A_{FB} angular parameters, as:

$$\frac{1}{d\Gamma/dq^2} \frac{d^3\Gamma}{dq^2 d\cos\theta_l d\cos\theta_K} = \frac{9}{16} \left[\frac{1}{2} (1 - F_L) (1 - \cos^2\theta_K) (1 + \cos^2\theta_l) + 2F_L \cos^2\theta_K (1 - \cos^2\theta_l) + \frac{4}{3} A_{FB} (1 - \cos^2\theta_K) \cos\theta_l \right] \quad (1)$$

The q^2 spectrum, ranging from 1 to 19 GeV^2 , has been divided in 5 bins, and the values of the angular parameters are measured independently in each q^2 bin. The q^2 bins $8.68 < q^2 < 10.09 \text{ GeV}^2$ and $12.89 < q^2 < 14.18 \text{ GeV}^2$, contain the $B^0 \rightarrow K^{*+}J/\psi$ and $B^0 \rightarrow K^{*+}\psi(2S)$ decays, respectively, and are used as control channels to validate the analysis. In addition the analysis is repeated in a special bin covering the whole q^2 spectrum excluding the two bins of the control regions.

The angular parameters A_{FB} and F_L are extracted from a three-dimensional unbinned extended maximum-likelihood fit to the B^+ candidate mass, m , the $\cos\theta_K$, and the $\cos\theta_\ell$ distributions, in each q^2 range. The probability density function (pdf) used in the fit is:

¹The result presented here is in line with what was presented at the conference. An update of this result is available [6].

$$\begin{aligned} \text{p.d.f.}(m, \cos \theta_\ell, \cos \theta_K) = & Y_S \cdot S^m(m) \cdot S^a(\cos \theta_\ell, \cos \theta_K) \cdot \epsilon(\cos \theta_K, \cos \theta_\ell) \\ & + Y_B \cdot B^m(m) \cdot B^{\theta_\ell}(\cos \theta_\ell) \cdot B^{\theta_K}(\cos \theta_K) \end{aligned} \quad (2)$$

where the two contributions correspond to the parametrisation of the signal and background. The Y_S and Y_B parameters are the yields of signal and background events, respectively. The functions $S(m)$ and $S^a(\cos \theta_\ell, \cos \theta_K)$ describe the signal invariant mass and angular distributions, while $B^m(m)$, $B^{\theta_\ell}(\cos \theta_\ell)$ and $B^{\theta_K}(\cos \theta_K)$ functions describe the background distributions.

The function $\epsilon(\cos \theta_\ell, \cos \theta_K)$ encodes the signal efficiency as a function of the angular variables. The efficiency function is composed as:

$$\epsilon(\cos \theta_K, \cos \theta_\ell) = \varepsilon_{1D}(\cos \theta_K) \cdot \varepsilon_{1D}(\cos \theta_\ell) \cdot [1 + C(\cos \theta_K, \cos \theta_\ell)] \quad (3)$$

where $\varepsilon_{1D}(\cos \theta_K)$ and $\varepsilon_{1D}(\cos \theta_\ell)$ are two one-dimensional functions, which are parameterised either as polynomials or as sum of Gaussian functions, according to the q^2 bin, and $C(\cos \theta_K, \cos \theta_\ell)$ is a two-dimensional functions parameterised as a product of polynomials and Legendre polynomials. The efficiency function is determined on simulated Monte Carlo (MC) events, with a two step procedure: firstly the parameters of the one-dimensional functions are determined by fitting separately the projections of the MC sample on the two angular parameters; then, while the parameters of the one-dimensional functions are kept fixed, the ones of the $C(\cos \theta_K, \cos \theta_\ell)$ function are determined by fitting the two-dimensional distribution of the MC sample with the $\epsilon(\cos \theta_K, \cos \theta_\ell)$ function, to correctly account for correlations between the two variables.

The signal mass shape $S(m)$ is modelled as the sum of two Gaussian functions with a common mean, which are determined by a fit to the mass distribution of the MC events. The angular shape $S^a(\cos \theta_\ell, \cos \theta_K)$ is given in Equation (1). The background mass shape $B^m(m)$ is modelled as a single exponential function, while the background angular shape $B^{\cos \theta_\ell}(\cos \theta_\ell)$ is parameterised as a combination of Gaussian function, exponential functions, or a polynomial, depending on the q^2 bin.

The fit to the data is performed in two steps: firstly the parameters of the background angular functions are determined (and fixed in the second step) by fitting the distribution of the events in the mass sidebands; then, all the events in the data sample are fitted, to determine the yields, Y_S and Y_B , the angular parameters, A_{FB} and F_L , and the exponential decay parameter of $B^m(m)$.

The fitting procedure has been validated using MC simulated samples. The statistical uncertainty on the A_{FB} and F_L results has been determined using a profiled Feldman-Cousins method, to ensure a correct coverage.

Several sources of systematic uncertainties are considered in this analysis, which are related to the effect of the statistical fluctuations of the MC sample and of data/MC differences on the efficiency modelling, the effects of a possible contamination of S-wave $\pi^+K_s^0$ pairs, and the effect of a bias in the background angular parametrisation. The dominant systematic uncertainty is the one related with the background parametrisation and is composed as the sum in quadrature of three effects: the propagation of the statistical uncertainty of the fit to the data sidebands, the effect of choosing a smaller sideband range of definition, and the effect of choosing different functions to model the background angular shape.

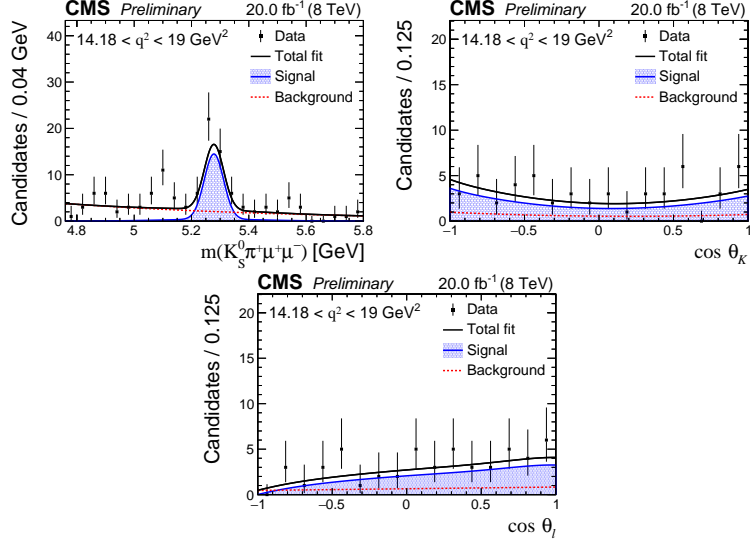


Figure 1: The fitted B^+ invariant mass, m , (left) and the angular variables $\cos \theta_K$ (centre) and $\cos \theta_\ell$ (right) for the events in the signal region $5.18 < m < 5.38$ GeV, for $14.18 < q^2 < 19$ GeV². The filled area, dashed lines, and solid lines represent the signal, background, and total contributions, respectively. The vertical bars represent the statistical uncertainty. Figure from [5].

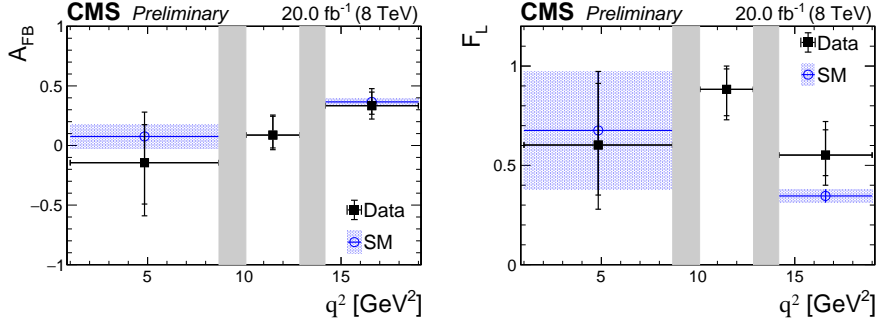


Figure 2: The measured values of A_{FB} and F_L versus q^2 for $B \rightarrow K^{*+}\mu^+\mu^-$ decays. The statistical (total) uncertainty is shown by inner (outer) vertical bars. The vertical shaded regions correspond to the $B \rightarrow K^{*+}J/\psi(\mu^+\mu^-)$ and $B \rightarrow K^{*+}\psi(2S)(\mu^+\mu^-)$ dominated regions. The blue band shows the SM predictions for the corresponding q^2 range. Figure from [5].

The projections of the fit results for the $K^{*+}\mu^+\mu^-$ invariant mass distribution and of the $\cos \theta_K$ and $\cos \theta_\ell$ distributions for the events in correspondence of the mass peak, for the bin at high q^2 , are shown in Figure 1. The systematic and statistical uncertainties are added in quadrature to obtain the total uncertainty.

The measured values of A_{FB} and F_L are shown in Figure 2. The uncertainties are dominated by the statistical errors. The results are consistent with the SM predictions [7].

3. Prospects for $B^0 \rightarrow K^{*0}\mu^+\mu^-$ analysis at CMS during High-Luminosity LHC

The High-Luminosity LHC (HL-LHC) run is expected to deliver about 3 ab^{-1} of integrated luminosity, in pp collisions at centre of mass energy of 14 TeV [8]. Relevant improvements of the

CMS detector are planned for HL-LHC [9], in order to efficiently acquire data in its challenging operation conditions. In particular, a silicon detector with extended rapidity coverage, improved granularity, and higher radiation tolerance will be installed. This is expected to provide a significant improvement in the mass-measurement resolutions, and a better signal-over-background ratio in the reconstructed decay channels.

Using the result of the CMS analysis on 2012 data [3] as baseline, a study has been performed to estimate the expected precision of the measurement of one of the angular parameters of the $B^0 \rightarrow K^{*0}\mu^+\mu^-$ angular distribution, P'_5 , at the integrated luminosity of 3 ab^{-1} [10]. For simplicity, in this study the signal-to-background ratio and the trigger thresholds and efficiencies are assumed to be unchanged with respect to the 2012 analysis, and effects of possible improvements in the analysis strategy have not been considered.

Samples of simulated signal events with Phase-2 conditions, which account for the foreseen upgrades to the CMS detector, are used. In each q^2 bin, the signal yield is extracted performing a maximum likelihood fit to the B^0 -candidate mass spectrum, and extrapolating to an integrated luminosity of 3 ab^{-1} . The statistical uncertainty and the systematic uncertainties that are directly dependent on data statistics are obtained by scaling the correspondent uncertainties from the 2012 analysis by the square root of the 2012 over HL-LHC signal-yield ratio. The other systematic uncertainties are scaled by a factor of 2. Overall, the uncertainties are reduced down to a factor of 15 compared to the 2012 results, as shown in Figure 3. Since these projected results are dominated by the systematic uncertainties, finer q^2 bins could be used with no relevant degradation of the precision of the measurements. An additional study has been performed, by splitting some of the q^2 bins in finer bins such that the statistical and systematic uncertainties are approximately equal, as shown in the bottom pads of Figure 3.

4. Conclusions

The results of the angular analysis performed for the decay of $B^+ \rightarrow K^{*+}\mu^+\mu^-$, using pp collision data recorded at $\sqrt{s} = 8 \text{ TeV}$ with the CMS detector corresponding to an integrated luminosity of 20.5 fb^{-1} , are presented here. In each region of the dimuon invariant mass squared, unbinned maximum-likelihood fits are applied to the distributions of the B meson invariant mass and the angular variables, to extract the values of the fraction of longitudinally polarised K^{*+} and of the muon forward-backward asymmetry. The results are consistent with the predictions from the Standard Model. Finally, the projections for the sensitivity of the measurement of the P'_5 parameter in the $B^0 \rightarrow K^{*0}\mu^+\mu^-$ angular analysis at the High-Luminosity LHC has been presented.

References

- [1] CMS Collaboration, JINST 3 S08004 (2008)
- [2] V. Khachatryan *et al.* [CMS Collaboration], Phys. Lett. B **753** (2016), 424-448
doi:10.1016/j.physletb.2015.12.020 [arXiv:1507.08126 [hep-ex]].
- [3] A. M. Sirunyan *et al.* [CMS Collaboration], Phys. Lett. B **781** (2018) 517
doi:10.1016/j.physletb.2018.04.030 [arXiv:1710.02846 [hep-ex]].

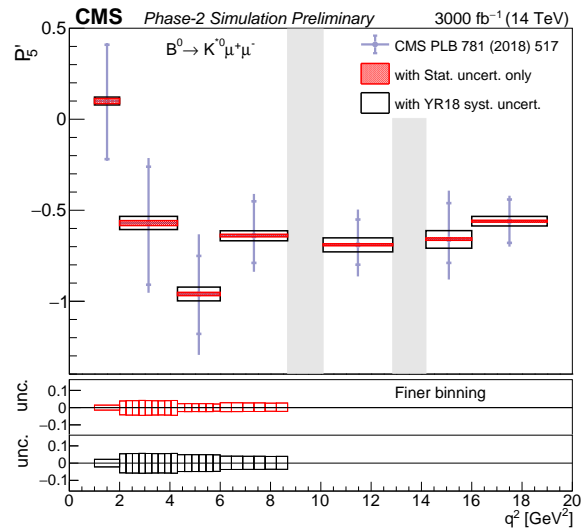


Figure 3: Projected statistical (hatched regions) and total (open boxes) uncertainties on the P'_5 parameter versus q^2 in the Phase-2 scenario with an integrated luminosity of 3000 fb^{-1} . The CMS measurement of P'_5 on 2012 data is shown by circles with inner vertical bars representing the statistical uncertainties and outer vertical bars representing the total uncertainties. The vertical shaded regions correspond to the J/ψ and ψ' resonances. The two lower pads represent the statistical (upper pad) and total (lower pad) uncertainties with the finer q^2 binning. Figure from [10].

- [4] A. M. Sirunyan *et al.* [CMS Collaboration], Phys. Rev. D **98** (2018) 112011
doi:10.1103/PhysRevD.98.112011 [arXiv:1806.00636 [hep-ex]].
- [5] A. M. Sirunyan *et al.* [CMS Collaboration], CMS-PAS-BPH-15-009,
<https://cds.cern.ch/record/2725506>.
- [6] A. M. Sirunyan *et al.* [CMS Collaboration], CMS-BPH-15-009,
<https://cds.cern.ch/record/2742836> [arXiv:2010.13968 [hep-ex]].
- [7] S. Descotes-Genon, L. Hofer, J. Matias and J. Virto, JHEP **12** (2014), 125
doi:10.1007/JHEP12(2014)125 [arXiv:1407.8526 [hep-ph]].
- [8] G. Apollinari, I. Béjar Alonso, O. Brüning, P. Fessia, M. Lamont, L. Rossi and L. Taviani,
CERN Yellow Report CERN 2017-007-M doi:10.23731/CYRM-2017-004.
- [9] D. Contardo, M. Klute, J. Mans, L. Silvestris and J. Butler, report: CERN-LHCC-2015-010
<https://cds.cern.ch/record/2020886>.
- [10] CMS Collaboration, report: CMS-PAS-FTR-18-033 (2018)
<https://cds.cern.ch/record/2651298>.